Extended Abstracts of the 2015 International Conference on Solid State Devices and Materials, Sapporo, 2015, pp1064-1065

Embedded Source Field-Plate for Reduced Parasitic Capacitance of AlN/GaN MIS-HEMTs on Si Substrate

Kentaro Chikamatsu, Minoru Akutsu, Taketoshi Tanaka, Shinya Takado, Koki Sakamoto
Norikazu Ito, and Ken Nakahara

ROHM Co., Ltd.
21 Saiin Mizosaki-cho, Ukyo-ku, Kyoto 615-8585 Japan
Phone: +81-75-321-4318 E-mail: Kentaro.Chikamatsu@dsn.rohm.co.jp

Abstract

GaN-based MIS-HEMTs are fabricated with embedded source field-plate (ESFP) locating near the bottom area of gate by self-alignment process. The ESFP MIS-HEMTs realize a lower gate-to-drain capacitance and gate-to-source capacitance than those of GaN MIS-HEMTs with a gate field-plate (GFP). Hence an ESFP device has a total gate charge (Q_g) of 920 pC at gate-source voltage of 6 V in spite of a Q_g of 2.8 nC for a GFP device. As a result of which, the ESFP device exhibits shorter transient times in switching than the GFP device.

1. Introduction

The GaN-based metal-insulator-semiconductor high electron mobility transistor (MIS-HEMT) has been developed aiming at low gate and drain leakage current [1, 2], high threshold voltage (V_{th}) for high voltage [3, 4], and/or high frequency operation [5]. Many MIS structures adopt gate field-plate (GFP) structure, which involves gate electrodes extended toward drain electrodes (Fig.1 (a)), to avoid large electric field around gate. The GFP structure, however, hampers high frequency operations through accompanied large gate-to-drain capacitance (C_{gd}) and gate-to-source capacitance (C_{gs}), because the field plates introduce extra capacitance with 2 dimensional electron gas (2DEG) at AlGaN/GaN hetero-interfaces acting as counter electrodes. These additional capacitance results in high input capacitance (C_{iss}=C_{gs}+C_{gd}), inevitably leading to high total gate charge (Q_g). In general, GaN-based MIS-HEMTs have high potential of high frequency switching, and therefore engineers have to achieve as small Q_g as possible. In this paper, we propose GaN MIS-HEMTs with embedded source field plate (ESFP), and prove that these devices are capable of switching in shorter transient times than GFP devices.

2. Device structure and fabrication process

The unit-transistor structure of the fabricated AlN/GaN MIS-HEMTs with conventional GFP and our proposed ESFP are depicted in Fig.1 (a) and (b), respectively. The epitaxial layers with SiN passivation, grown by metal organic chemical vapor deposition, are the same for both devices as shown in the figures. A sheet carrier density, sheet resistance, and mobility of 2DEG were 1.4×10^{13} cm^{-2}, 382 Ω/□, and 1203 cm^{2}V^{-1}s^{-1}, respectively.

Mo were deposited just on passivation and partially etched off for ESFP. A 500-nm-thick SiO_2 film was formed on these Mo films as inter-metal dielectric (IMD) films to extend the gate electrode over the passivation films and well above the ESFP and 2DEG. Gate opening was patterned on the Mo films, followed by Mo etching off inside the gate opening. This process leads to self-aligned gate and ESFP. Gate trenches were fabricated and dielectric films were formed on sidewalls of the gate trenches in order to keep a certain distance between the gate electrode and the ESFP.

Source and drain electrodes, Ti/Al, were deposited and then annealed at 550 °C for 10 min in an N_2 ambient to form Ohmic contact, leading to a specific contact resistance of 3.02×10^5 Ωcm^2. The GaN cap and top AlN layer in gate region were fully oxidized. A 40-nm-thick SiO_2 gate dielectric film was formed by PECVD, followed by Mo gate electrode deposition. The basic device parameters are as follows: 1-μm gate length, 2-μm gate–source distance, 6-μm gate–drain distance, 0.5-μm gate and SFP length, and 9-cm total gate width.

Fig.2 shows the top view of an ESFP AlN/GaN MIS-HEMT. The chip size was 1.9 × 1.9 mm. The ESFP metals were connected to the source electrode by the source interconnection metals in the non-active region as displayed in the figure.

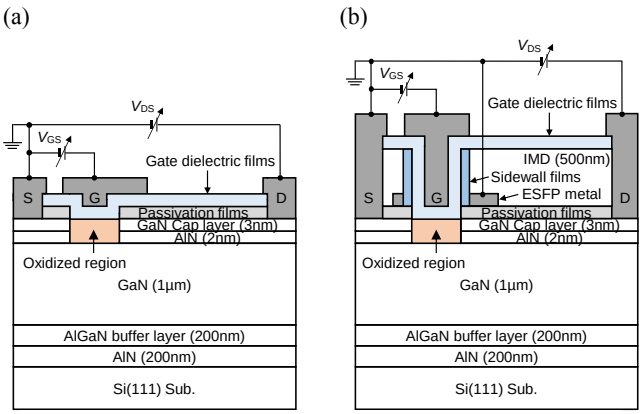

Fig. 1 Cross-sections of fabricated AlN/GaN MIS-HEMTs with (a) a conventional GFP and (b) an ESFP.

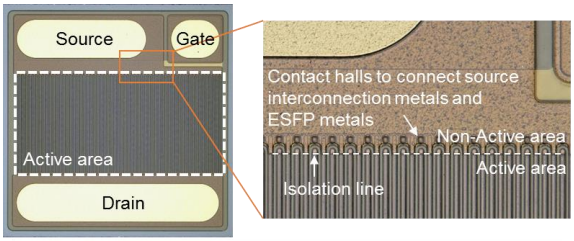

Fig. 2 The top view of an ESFP AlN/GaN MIS-HEMT.

3. Results and Discussion

All static- and dynamic-characteristic measurements were performed at room temperature under a substrate-source short circuit condition. Fig.3 (a) exhibits drain-source current (I_{DS}) – drain-source voltage (V_{DS}) characteristics of an ESFP GaN MIS-HEMT with Keysight B1505A power device analyzer. The device operated on E-mode to pinch off at a gate-source voltage (V_{GS}) of +0.6 V with the maximum I_d of 13 A and a static on-resistance (R_{on_static}) of 190 mΩ. Current collapse was evaluated by using B1505A. In this report, the current collapse factor (CCF) is defined as the dynamic on-resistance ($R_{on\_dynamic}$) divided by R_{on_static}, where the $R_{on\_dynamic}$ means here the R_{on} measured 100 µs after applying a certain stress bias to drain for 10 s with V_{GS} = 0 V. As shown in Fig.3 (b), the CCFs are better for ESFP devices than for GFP MIS-HEMTs.

The parasitic capacitances were measured at 1 MHz with B1505A, and differ between the ESFP and GFP structure. In GaN HEMTs, C_{gd} at V_{DS} = 0 V mainly originates from a capacitance comprising gate electrode and 2DEG. Our proposed ESFP structure, however, has the drain-side extension of the gate electrodes facing ESFP whose potential is fixed by source voltage, and thus reduces C_{gd}. Moreover, thick IMD films between the gate electrodes and 2DEG or ESFP are adopted to decrease C_{gs}. Therefore the C_{iss} and reverse transfer capacitance, C_{rss}(=C_{gd}), of the ESFP HEMTs are significantly smaller than those of the GFP MIS-HEMTs as shown in Figs.4, while the output capacitance (C_{oss}) stays unchanged. These small C_{gd} and C_{gs} lessen Q_g. One of our ESFP GaN MIS-HEMT has a Q_g of 920 pC at V_{GS} = 6 V, while the GFP GaN MIS-HEMT typically shows a Q_g of 2.8 nC.

Fig. 5 (a) depicts the circuit to estimate switching performance and (b) shows the waveforms of V_{GS} and V_{DS} of an ESFP GaN-MIS-HEMT at a switching frequency of 20 kHz. The results summarized in Table I clearly prove that our proposed ESFP significantly improves transient times. These facts also reflect the indigenous capability of GaN MIS-HEMTs for high frequency switching, if our proposed ESFP structure are adopted.

3. Conclusions

In this work, the team demonstrated AlN/GaN MIS-HEMTs with a novel ESFP. The ESFP structure reduces the parasitic capacitances of a device, especially in C_{gd}, compared to a conventional GFP structure. These small parasitic capacitances finally achieve very small switching transient times.

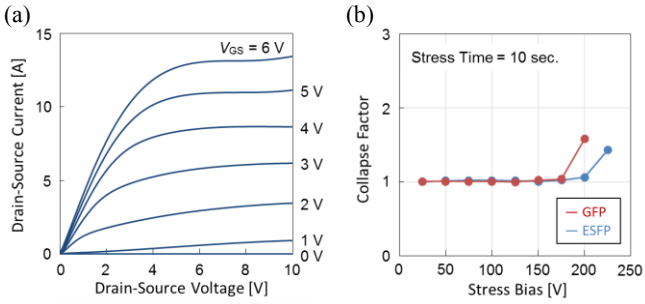

Fig. 3 (a) I_{DS}-V_{DS} characteristics and (b) CCF as a function of stress bias of AlN/GaN MIS-HEMTs with ESFP and GFP.

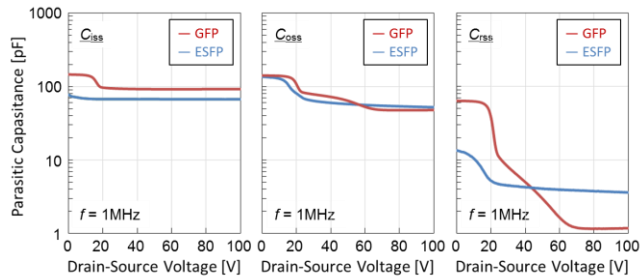

Fig. 4 Parasitic capacitance characteristics, C_{iss}, C_{oss} and C_{rss} of AlN/GaN MIS-HEMTs with GFP and ESFP.

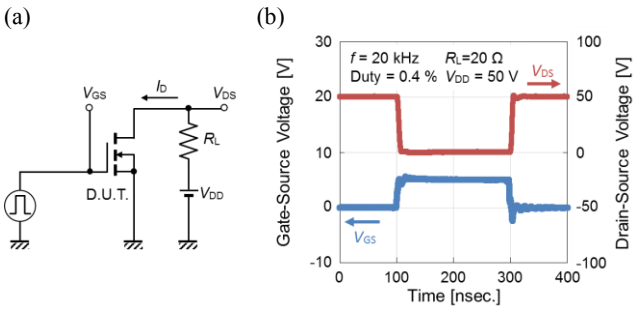

Fig, 5 (a) Switching measurement circuit and (b) switching waveforms of V_{GS} and V_{DS} of an ESFP AlN/GaN MIS-HEMT.

Table I Switching transient times of an ESFP GaN-MIS-HEMT.

Parameter	Symbol	ESFP	GFP
Turn-on delay time	$t_{d(on)}$	3.0 nsec.	3.2 nsec.
Rise time	t_r	4.5 nsec.	7.8 nsec.
Turn-off delay time	$t_{d(off)}$	4.0 nsec.	5.9 nsec.
Fall time	t_f	3.1 nsec.	5.2 nsec.

References

[1] H. Zhou *et al., Appl. Phys. Express.* 4 (2011) 104102.
[2] W. Choi *et al., IEEE Electron Device Lett.*, 35 (2014) 175.
[3] Y. Wang *et al., IEEE Electron Device Lett.*, 34 (2013) 1370.
[4] M. Kanamura *et al., IEEE Electron Device Lett.*, 31 (2010) 189.
[5] J. Kashiwagi *et al., IEEE Electron Device Lett* 34 (2013) 1109.